ISSN: 0974-5823 Vol. 7 No. 6 June, 2022

International Journal of Mechanical Engineering

FACILE GREEN MEDIATED SYNTHESIS AND TUNING OF DIELECTRICAL BEHAVIOR OF COBALT OXIDE NANOPARTICLES VIA Cu DOPING

A. Ajitha[1], K. Seethalakshmi[2], M. Meena[3]

[1,3]Department of Physics, S.T. Hindu College Nagercoil,

Affiliated to Manonmaniam Sundaranar University, Abishekapatti,

Tirunelveli - 627 012, Tamil Nadu, India.

[2]Department of Physics, Sree Devi Kumari Women's College, Kuzithurai,

Affiliated to Manonmaniam Sundaranar University, Abishekapatti,

Tirunelveli - 627 012, Tamil Nadu, India.

Abstract

We attempted to improve the electrical properties of cobalt oxide nanoparticles prepared using egg albumen via microwave assisted hydrothermal method by using copper as a dopant in various molar concentrations. [1, 3, and 5 mole%]. The structural evaluation of bare and doped samples were done using SEM analysis and X-ray diffraction. Egg albumen's role as a stabiliser and size controller is highlighted by the acquired topology and low average crystalline size. The dielectric constant and dielectric loss behaviour were measured between 40°C and 150°C for various frequency range. It is recommended to utilise both pure and doped Co_3O_4 as gate oxide materials for capacitors due to the high dielectric constant at low frequencies. Additionally, the fact that the dielectric constant and dielectric loss of the nanomaterial decrease as the frequency rises suggests that this nanomaterial might be used to make devices with high frequencies.

Key words: Co_3O_4 nanoparticles, Hydrothermal, Egg albumen, electrical studies.

1. Introduction

Metal oxide nanoparticles' potential technological applications are a major draw for researchers in the fields of materials chemistry, biology, medicine, agriculture, information technology, optical, electronics, catalysis, environment, energy, and senses. The substantial density and high surface to volume ratio of metal oxide nanoparticles are thought to be responsible for their special chemical and physical characteristics**.** Due to their distinct qualities, including great chemical stability, catalysis, electrical conductivity, and antibacterial activities, among others, cobalt oxide nanoparticles have drawn a lot of attention. [Guoru Lie et al., 2022][S Gopinath et al., 2022] [Luhan Wei etal.,2022].

As the need for non-toxic, secure, ecologically sustainable, and green processes increases the lot of attention towards green mediated preparation of Metal oxide NPs[R. Britto-Hurtado et al., 2022].It is possible to quickly, easily, cheaply, and effectively create the needed metal or metallic oxide nanoparticles using biological resources like plants and microbes. Therefore, employing green synthesis of nanoparticles promotes green chemistry ideas such as less risky chemical synthesis, safe

solvents and auxiliaries, energy-efficient design, and the use of renewable feedstocks[Mahmoud Abd El Aleem Ali El-Remaily et al., 2016].The creation of green synthesized nanoparticles using egg albumen is relatively uncommon, according to the pertinent literature review. Egg white is widely recognised for its ability to froth and emulsifying property because it is quickly soluble in water and readily reacts with metal ions. Furthermore, it's function as a gel or binder for substances used in moulding [P. AjiUdhaya and M. Meena., 2019]. Also, it is cost-effective and eco-friendly.According to many research findings, the pure Co_3O_4 nanoparticles made through green synthesis have very large particle size. Tahir Rasheed et al.,2019created cobalt oxide nanoparticles in a size range of 50 to 100nm. So egg albumin can be used to produce nanomaterials with controlled shape and narrow size distribution.With the inclusion of egg white, an facile technique for synthesising oxide approaches was found.

Elemental doping has recently become a popular and effective technique for improving the optical and electrical performance of metal oxide nanoparticles[KezhenQi et al.,2019].The most efficient method to improve Co_3O_4 nanoparticles' optical, electrical, magnetic, antibacterial, and photocatalytic properties is to dope them with metals and non-metals. The copper doped metal oxide nanoparticles have certain advantages, according to several research findings.Because of this, it is anticipated that the synergism from the combination of intrinsic and extrinsic Cu doping would be very intriguing in electrical applications and that it would attain much better performance than pristine Co_3O_4.

Due to the aforementioned reasons, we created cobalt oxide nanoparticles using the microwave assisted hydrothermal green technique with egg white and alsoto investigate, how the copper ion doping may impact the physical, optical, and electrical properties of the Co_3O_4 nanoparticles.

2. Synthesis

Pure and copper-doped Co_3O_4 nanoparticles were prepared using a simple microwave assisted hydro-thermal method via egg albumin. In the present study, cobaltacetate and egg albumin were used as precursors for the synthesis of pure and copper doped cobalt oxide nanoparticles. The precursors in the ratio of 1:3 were taken separately and dissolved in the solvent of distilled water. Freshly prepared egg albumin solution is added drop wise to cobalt acetate solution while it is constantly stirred.The final solution is then kept in a domestic microwave oven for about 30 minutes. During microwave irradiation, egg albumin decomposes to produce oxygen ions and also it act as oxygen source and as well as capping material. The solvent is completely evaporated, and colloidal precipitate was formed. This colloidal precipitate was washed several times with doubly distilled water and then dried. The dried sample was washed with acetone to remove the organic impurities, if any. Then the as synthesised powder samples were calcined at 700 °C for an hour. The same procedure was followed when copper was doped in the molar concentration of 0.01, 0.03, and 0.05.

3. Instrumentation

Shimadzu's X-ray diffractometer, monochromated with CuK radiation in the 2θ range of 10 to 80 ° at a 10 ° per minute scan rate, has been used to obtain PXRD patterns for calcined materials.With the help of a field-emission scanning electron microscope, the structure morphology was studied (GEM-300, Carl Zeiss, Germany).The powdered materials were formed into pellets, and the AGILENT 4284 A was used to detect the dielectric parameters in various frequency range at different temperature using Two-probe method..

4. Results and Discussion

4.1 Structural Characterization using XRD

Fig..1 shows the recorded PXRD pattern of both bare and Cu-doped Co_3O_4.The bare Co_3O_4 nanoparticles' diffractogram closely resembles the diffraction peak at 2θ values of 19.03°, 31.21°, 36.9°, 38.55°, 44.9°, 55°, 59.35°, 65.4°, 68.76°, 69.78°, 77.9°, 78.38°, which corresponds to (1 1 1), (2 2 0), (3 1 1), (2 2 2), (4 4 0), (5 3 1), (4 4 2), (5 3 3), (6 2 2) crystal planes, respectively, in the standard spectrum of face-centred cubic crystalline Co_3O_4 as per JCPDS card number (# 43-1003).Copper inclusion results in a smaller peak shift in the diffraction pattern.With the rise in Cu concentrations, no additional peaks connected to the impurity phase were discovered, proving that the phases are stable and that Cu ions are uniformly incorporated inside the Co_3O_4 lattice.The intensity of diffraction peaks and crystallinity decrease with increasing copper content, possibly as a result of the strain created in the Co_3O_4 lattice due to the inclusion of Cu ions, which is well in agreement with the results reported by [Faniband, S. Met al., 2022][10][Muslima Zahan & Jiban Podder.,2022][Z. Sekhi Mehrabadi et al., 2011].

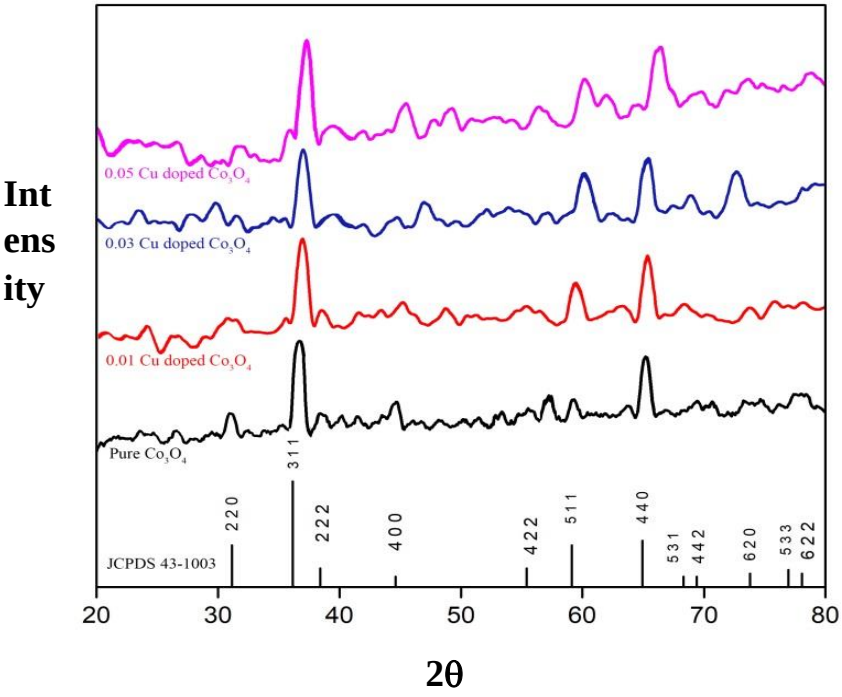

Fig. 1. X-ray diffractogram of bare and Cu doped Co_3O_4nano particles

Using the Debye-Scherrer formula, the average crystalline size of the proposed samples were determined [Selvanayaki R et al., 2022]. Unit cellWin software was used to calculate the lattice parameters, and the calculated values and the resultant crystalline size were tabulated in Table 1.

Table: 1. Unit cell parameter for pure and Cu-doped Co_3O_4 derived from the XRD pattern.

Sample	Pristine	Cu 0.01	Cu 0.03	Cu 0.05
Lattice parameter a (Å) (±0.009)	8.10	8.09	8.08	8.07
Volume V($Å^3$) (±1.8)	531.20	529.77	528.49	526.96

Crystallite size D(nm) (±3.07)	20.45	16.74	15.63	13.04
Average strain x 10^{-3} (± 0.5)	1.55	1.87	2.23	2.71
Dislocation density x 10^{-12} (±1.3)	3.20	3.67	4.1	6.26
Particle size D (nm) From SEM Histogram	24	21	16	15

Cu ions were quantitatively substituted in the lattice site as evidenced by the decreasing unit cell volume of Cu-doped pure Co_3O_4 with increasing concentration. Dislocation densities exhibit aberration as dopant concentrations increase.Table.1 shows that the dislocation rises as Cu doping concentration increases, indicating that Cu caused defects in the Co_3O_4 matrix. Decrease in crystallinity was caused by the creation of stress and lattice contraction [I.S. Okeke et al., 2021]. The modification of the lattice constant caused by the addition of Cu dopant to metal oxide nanoparticles may be the cause of crystal defects [Arshad et al., 2015].In nanoparticles, as size decreases, an increasing number of surface and interface atoms cause strain or stress as well as related to structural defects[Bansal V et al., 2006].

4.2 SEM Analysis

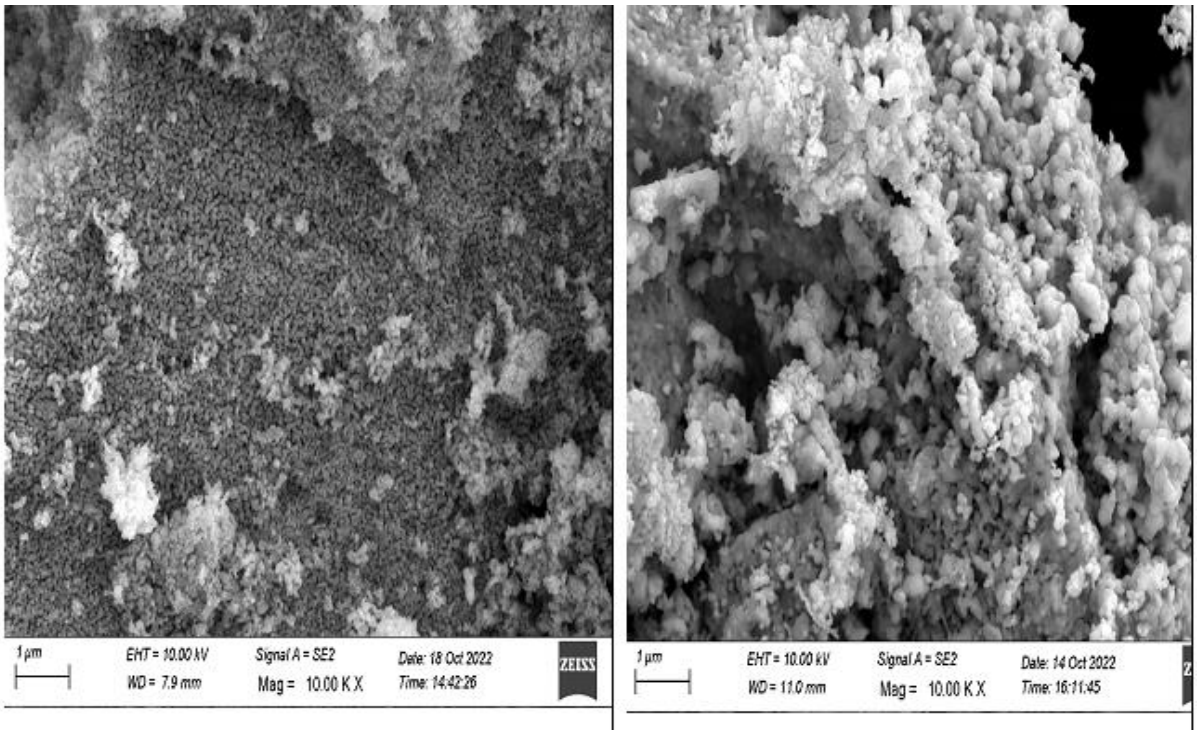

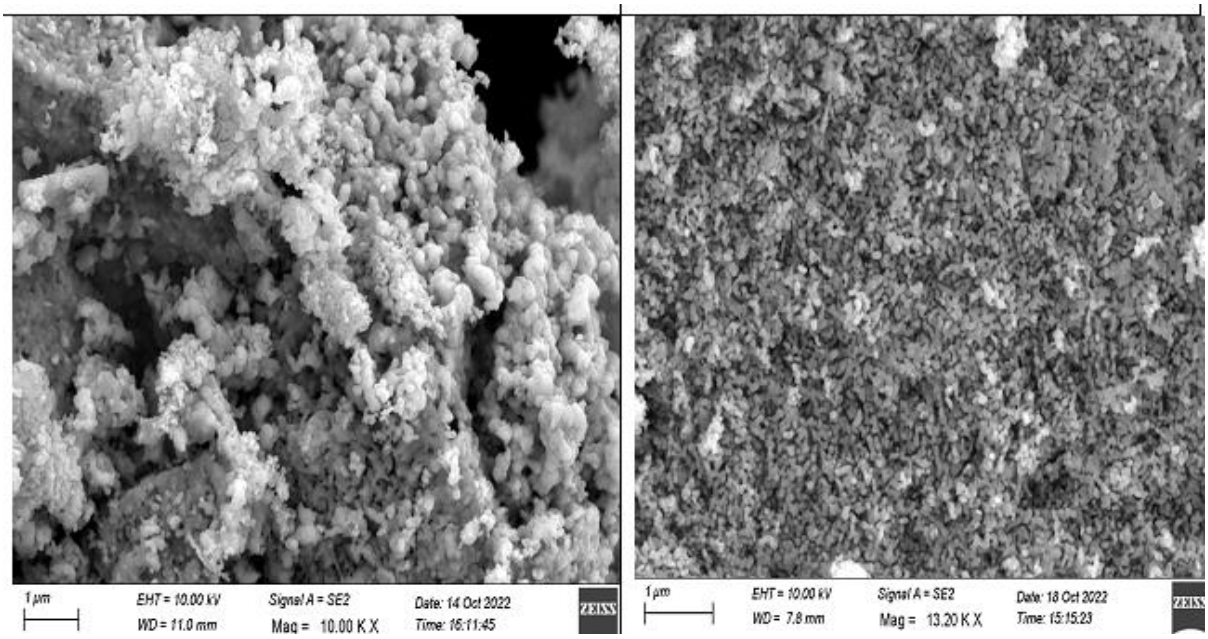

Fig. 2. SEM images of a) Pure Co_3O_4 b) 0.01 Cu doped Co_3O_4 c) 0.03 Cu doped Co_3O_4 d) 0.05 Cu doped Co_3O_4

Fig. 2 shows SEM images of cobalt oxide nanoparticles that are both pure and doped with copper. To ascertain the morphological characteristics of the framed copper-doped and bare cobalt oxide nanoparticles, SEM examination is employed.SEM images demonstrate the nanoparticles' size reduction.All calcined Co_3O_4 nanoparticles are examined using high-magnification SEM micrographs to evaluate their shape and grain size. A bunch-like structure was formed when the microscopic particles linked together, as can be seen in the greatly enlarged micrograph.The bunch-like structure changed as the Cu content rose, resulting in the emergence of denser formations. Clusters form, demonstrating that as concentrations rise, the strain also rises.Synthesised nanoparticles' crystalline nature is revealed by SEM analyses.

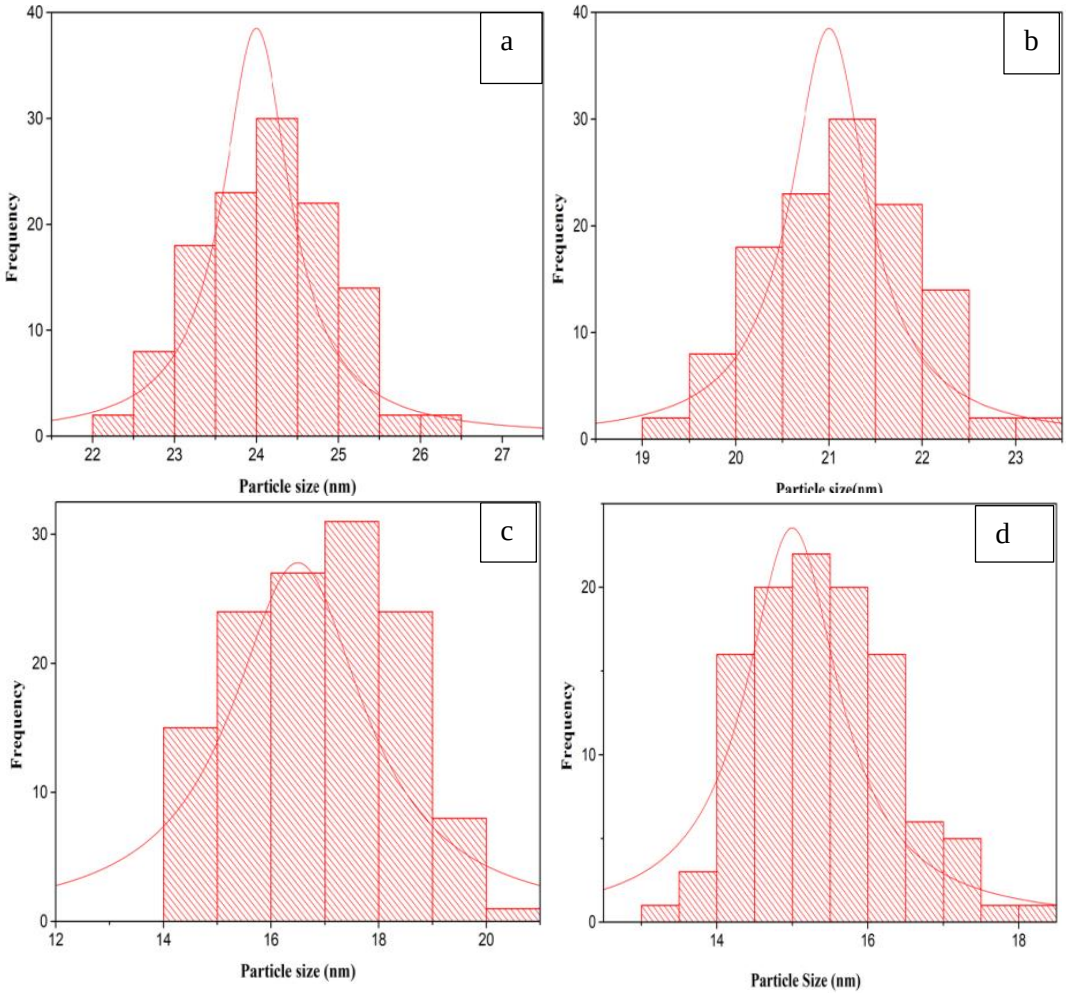

Fig..3. Particle size histogram of a) Pure Co_3O_4 b) 0.01 Cu doped Co_3O_4 c) 0.03 Cu doped Co_3O_4 d) 0.05 Cu doped Co_3O_4

Fig. 3. Shows the particle size histogram of pure and cu doped samples obtained from SEM using Image J software. The histogram above shows that as the amount of copper dopant is raised, the particle size of the produced nanoparticles decreases. An average particle size of the pure and Cu doped (0.01 %, 0.03 % and 0.05 %) Co_3O_4NPs were calculated as 24 nm, 21 nm, 16 nm and 15 nm which were correlated with XRD analysis. At 5 mole % doped sample, size distribution is very much narrow in the range of 14- 16 nm.

4.3. ELECTRICAL STUDIES

The pure and copper-doped Co_3O_4 nanoparticles were pelletized and electro-coated with carbon on both sides to make the electrical contact work as a parallel plate capacitor. Using an LCR meter to determine the capacitance and dissipation parameters, the dielectric constant and dielectric loss of the nanoparticles were estimated. In order to evaluate the frequency dependent dielectric properties of generated pure and Cu doped (0.01 mol, 0.03 mol, 0.05 mol) cobalt oxide nanoparticles, a frequency range of 1 KHz to 1 MHz and temperatures ranging from 40 to 150 °C were used.

Dielectric constant

The dielectric constant, an electrical characteristic, provides details about the atoms, ions, and their polarisation. The real part of the dielectric constant was calculated using the relationship [P. AjiUdhayaa, M. Meena., 2019].

$$\varepsilon'' = \frac{Cp \times t}{A \times \varepsilon 0}$$

Where A is the area of the sample and t is the thickness of the sample and $C_p$is the capacitance values

And using the relationship, the imaginary portion of the dielectric constant was determined.

$$\varepsilon''=\varepsilon' \tan\delta$$

For bare and Cu doped Co_3O_4, Fig. 4 to Fig. 7 illustrate the fluctuation of the real and imaginary parts of the dielectric constant (ε' and ε'') as a function of frequencies and temperature.Similar behaviour is displayed in the frequency-dependent fluctuation of the real and imaginary dielectric constant values. The dielectric constant is shown in Fig. 4 and 6 to be high at lower frequencies.With an increase in frequency, the values of the dielectricconstant are found to drop.It is possible to explain why the dielectric constant drops with the applied field using polarisations such as ionic, orientation, and electronic.The dielectric constant decreases as frequency increases as a result of the transition from interfacial to dipolar polarity.The biggest contribution to the dielectric constant originates from interfacial polarisation, while the others are quite small. The obtained samples have a high dielectric constant at low frequencies, which makes them suitable for the creation of capacitive pressure and bending sensors [N. Pereira et al., 2021].Materials with high dielectric constants are under intense investigation to improve dielectric constants and reduce the loss tangent (tanδ) for a variety of applications, including as energy-storage devices, microelectronic devices, and electromagnetic interference shielding devices[Z.-M. Danget al., 2012]. In the high frequency region, the dipoles will hardly be able to place themselves in the direction of the applied field, which causes the dielectric constant to decrease [M Meena et al., 2014]. In the high frequency domain, dipolar polarisation contributes as the dominant contributor because interfacial polarisation fails [Anantha et al., 2012]. The dielectric constant is frequency independent at higher frequencies because the alternating applied electric field's rapid variation is too quick for electric dipoles to follow [Sadaf Bashir Khan et al., 2019]. Nanostructured materials have a high aspect ratio in comparison to bulk materials, which causes more interfacial atoms and defects at the grain borders [NusratJahan., et al 2021][K.M. Batoo et al., 2020].

From fig. 5 and 7 As temperature and dopant concentration rise, the dielectric constant rises as well.The increase in temperature causes the charge carriers to get excited and have enough energy to follow changes in the applied field, which raises the dielectric constant [Gouda et al., 2009]. When the temperature is quite low, the charge carriers are in a low energy state. Due to the difficulty of moving the charge carriers and the tiny amount of movement that follows the direction of the applied field, polarisation and dielectric behaviour are only slightly affected [ChunYen et al. 2011].

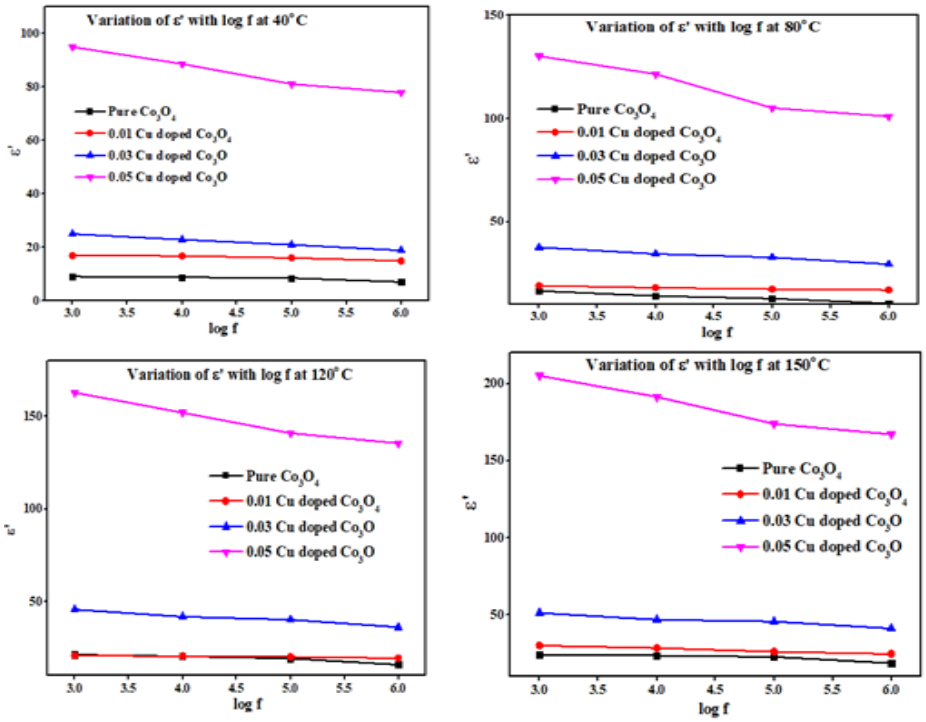

Fig.4. Variation of ε' of pure and Cu doped Co_3O_4 with log frequency at different temperatures

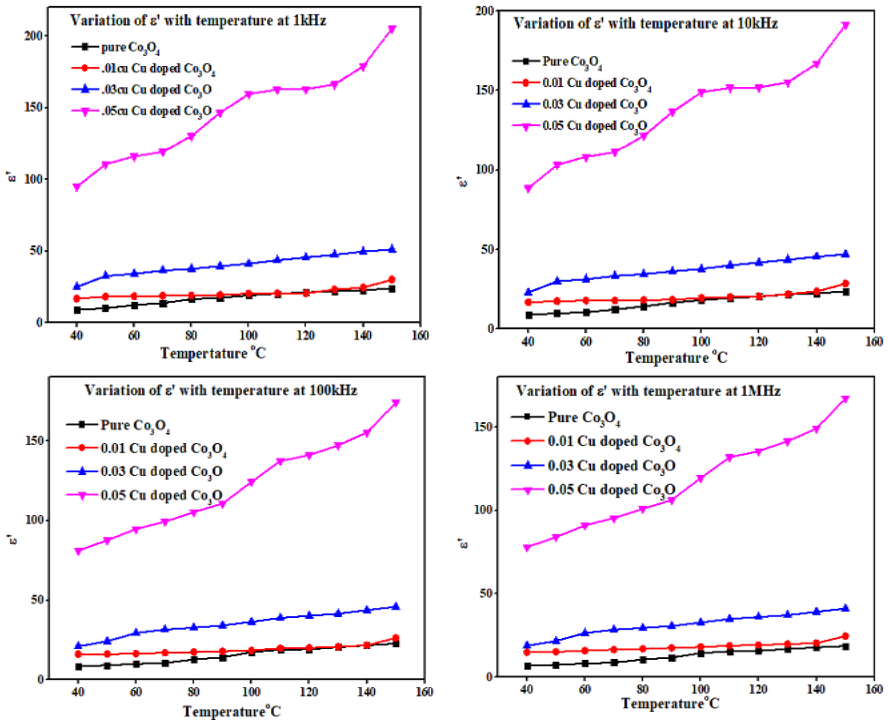

Fig.5. Variation of ε' of pure and Cu doped Co_3O_4 with temperature at different frequencies

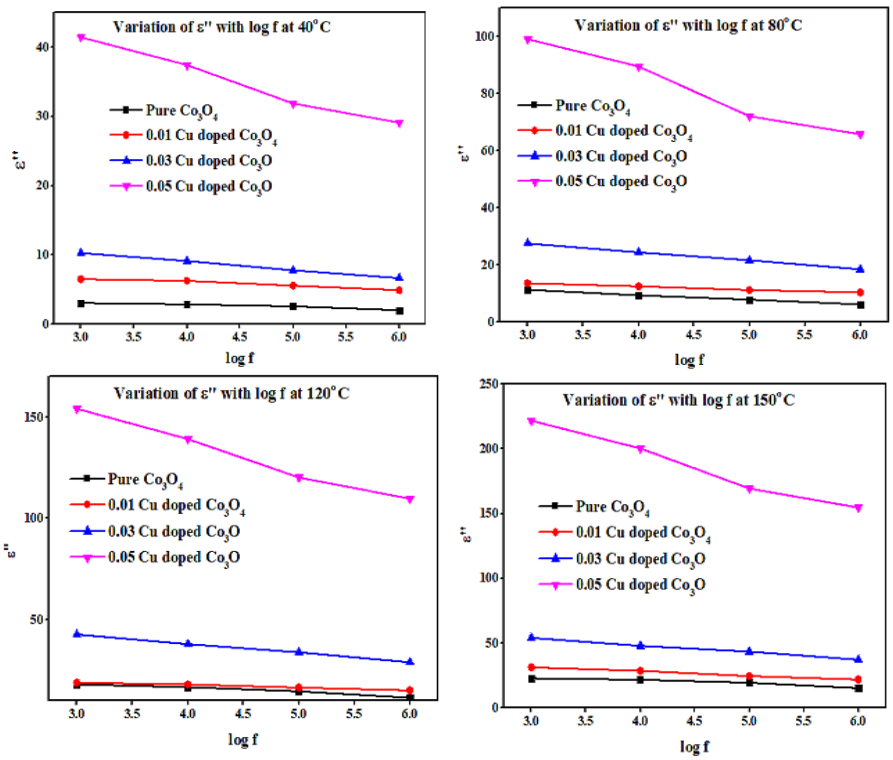

Fig.6. Variation of ε'' of pure and Cu doped Co_3O_4 with log frequency at different temperatures

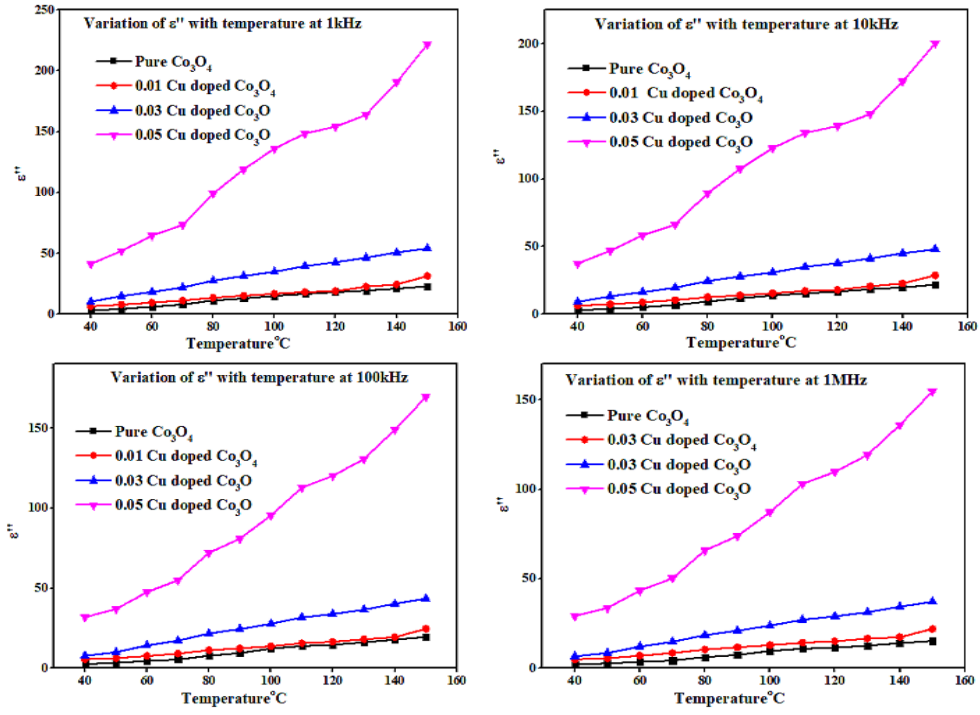

Fig.7. Variation of ε'' of pure and Cu doped Co_3O_4 with temperature at different frequencies

Dielectric loss factor

We deduced from Fig. 8 that for all frequencies, loss factor rises with both temperature and dopant concentration. Our investigation shows that the dielectric loss rises with temperature and dopant concentration while falling with frequency.The crystal structure and defects in the crystal system, such as impurities, grain boundaries, porosity, and random crystallite orientation, are attributed for the dielectric losses. Therefore, it is clear from the growing loss factor as Cu dopant concentration increases that the lattice is changed by the addition of Cu impurities by causing imperfections in the Co_3O_4 lattice. So increasing loss factor with increasingconcentration of the dopants evident that added impurities alters the lattice by producing imperfections in Co_3O_4 lattice. Therefore, it is clear from the rising loss factor with rising dopant concentration that the addition of impurities modifies the lattice by causing flaws in the Co_3O_4 lattice.According to our findings, the dielectric loss reduces with increasing frequency.Reduction in dielectric loss was compatible with the Debey type of relaxation method [M.A. Dar et al., 2010].The fact that the nanomaterial's dielectric constant and dielectric loss both decreased as the frequency increased suggests that this nanomaterial might be used to create devices with high frequency applications[M. M. El-Desoky et al 2016]. The values of tanδ are very low at higher frequencies, demonstrating the suitability of the material for high frequency microwave devices [H. Chouaibi et al., 2021].

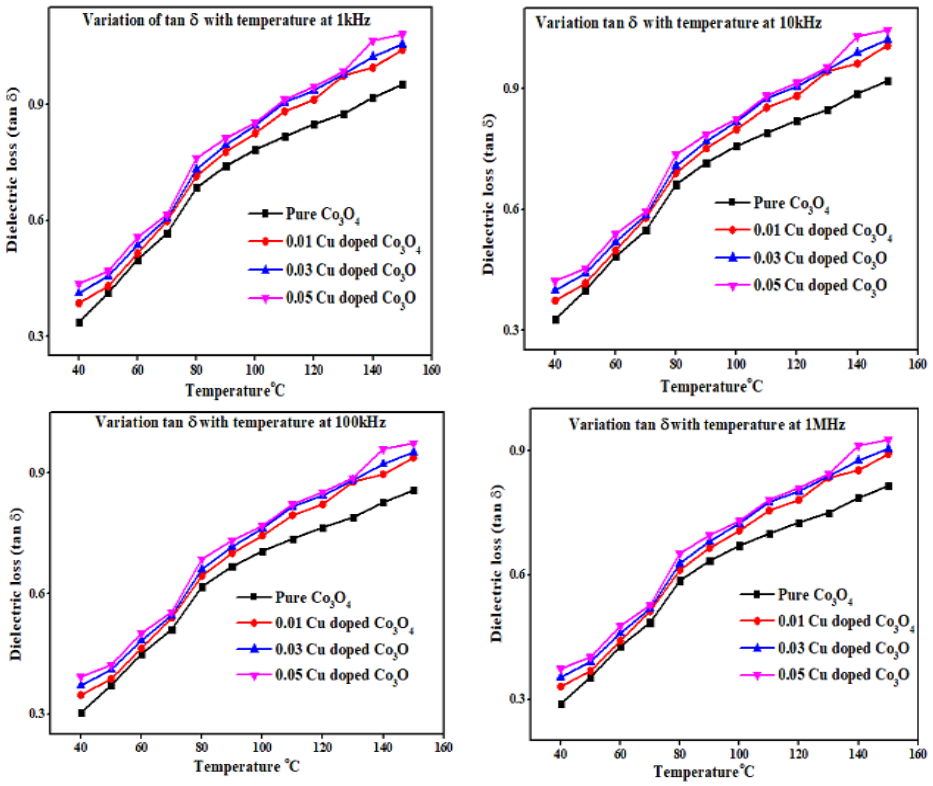

Fig.8. Variation of dielectric loss of pure and Cu doped Co_3O_4 with temperature at different frequencies

AC conductivity

The experiment consisted of determining the variations in AC conductivity (AC) with frequency ((ω=2πf) and temperature for both pure and copper-doped NPs at a range of temperatures between 303 K and 403 K (40 C and 150 C).

The method described below was used to calculate the electrical conductivity.

$\sigma_{ac} = \omega\varepsilon' \tan\delta\varepsilon_0$

where tanδ is the loss tangent, ε' is the dielectric constant, and ε_0 is the vacuum dielectric constant of 8.85×10^{-12} F/m.

Fig. 9 and 10 show the variation of conductivity with different frequencies and different temperatures. It is obvious that the AC electrical conductivity increases with frequency. As frequency increases, there is more hopping between charge carriers, which results in a higher AC conductivity rating. According to Fig. 9 and 10, conductivity increases along with a rise in dopant concentration. When Cu ions were added to Co_3O_4 nanoparticles, the concentration of mobility charge carriers and conductivity increased. As the mole percentage of Cu dopant increases, the electrical conductivity of the Co_3O_4 samples rises. The conductivity rises as the temperature rises, as shown in Fig. 9. The overall conductivity rises with temperature due to thermal agitation and an increase in the number of charge carriers [R. SakthiSudarSaravanan, M. Meena et al.,2014]. The increasing of AC electrical conductivity with temperature and frequency provides evidence for polaron hopping process.Because the hopping mechanism cannot vary in response to the applied ac field, the conductivity of the samples becomes invariant at high frequencies [T. Dippong et al., 2019].

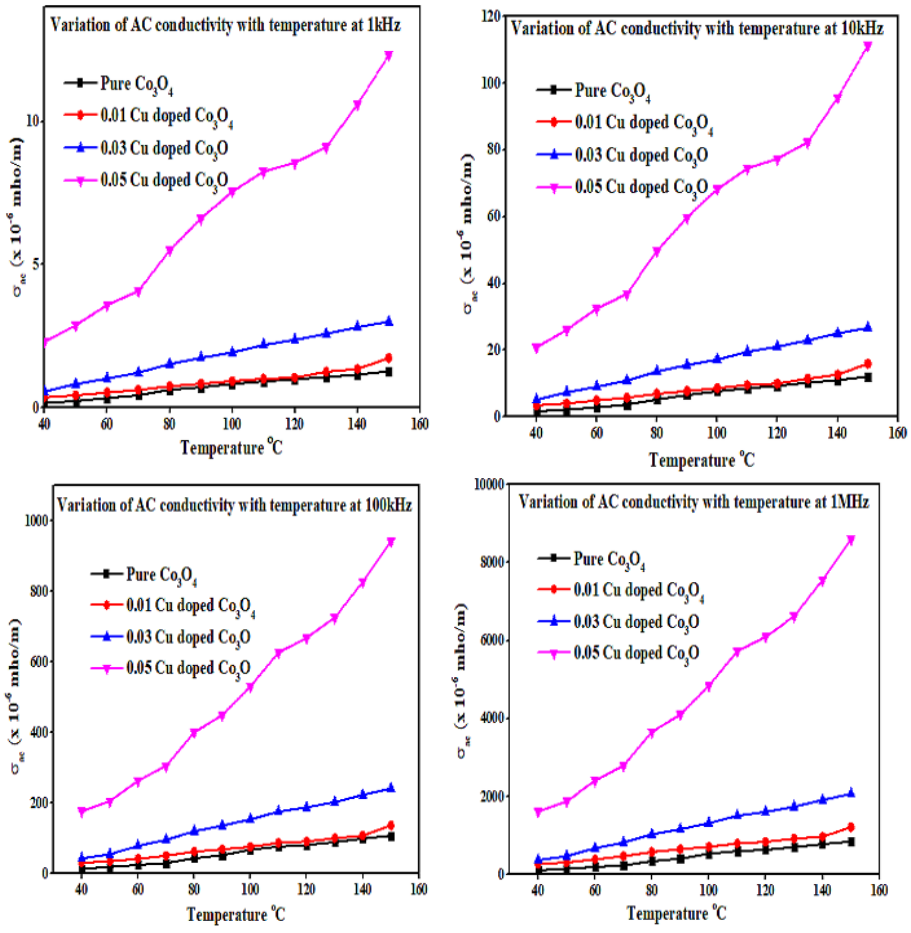

Fig.9.Variation AC conductivity of pure and Cu doped Co_3O_4 with temperature at different frequencies

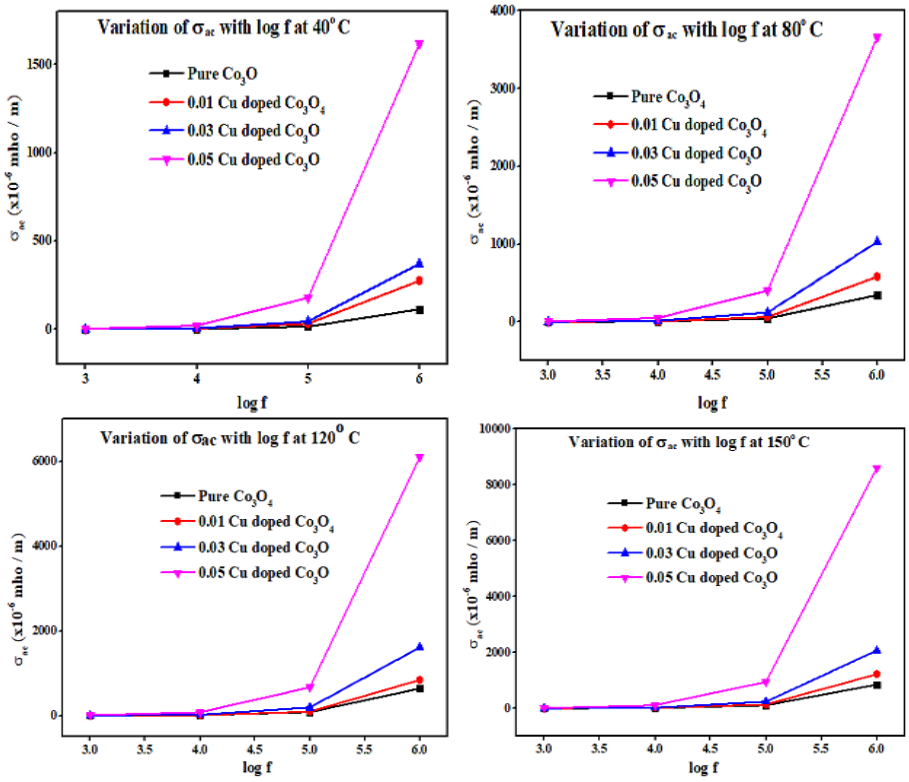

Fig.10.Variation of AC Conductivity of pure and Cu doped Co_3O_4 with log frequency at different temperatures

5. Conclusion

Using green synthesis, the bare and Cu-doped Co_3O_4 nanoparticles were effectively produced using microwave assisted hydrothermal method. The produced samples were put through structural, morphological, and electrical evaluations.The egg white protein albumen has acted as shaping agent and size controller in the preparation method. With an increase in applied signal frequency, the particle's dielectric constant and dielectric loss reduce, whereas an increase in frequency causes the AC conductivity to rise.The fact that the generated samples have a high dielectric constant indicates that they were used to make capacitive pressure and bending sensors. Also the high value of dielectric constant at low frequencies suggest the use of pure and doped Co_3O_4 as gate oxide materials for capacitors.

References

1. Guoru Li, Fengxiang Yin, Zhiping Lei, Xinran Zhao, Xiaobo He, Zhichun Li, Xiaoting Yu, Se-doped cobalt oxide nanoparticle as highly-efficient electrocatalyst for oxygen evolution reaction, International Journal of Hydrogen EnergyVolume 47, Issue 1, 1 January 2022, Pages 216-227, https://doi.org/10.1016/j.ijhydene.2021.10.001.2
2. S Gopinath, M. Mayakannan, S. Vetrivel, Structural, Optical, morphological properties of silver doped cobalt oxide nanoparticles by microwave irradiation method, Ceramic International, march 2022 pages 6103-6115, https://doi.org/10.1016/j.ceramint.2021.11.149.
3. Luhan Wei, Jianmin Wang, Zhen Zhao, Xi Yang, Sichen Jiao, Feng Cao, Shuai Tang, Xuefeng Zhang, Gaowu Qin, Qinghua Liang , Song Li, Co/Co_3O_4 nanoparticles embedded into thin O-doped graphitic layer as bifunctional oxygen electrocatalysts for Zn-air batteries, Chemical Engineering JournalVolume 427, 1 January 2022, 130931, https://doi.org/10.1016/j.cej.2021.130931.
4. R. Britto-Hurtado, M. Cortez-ValadezGreen Functionalized Nanomaterials for Environmental Applicationshttps://doi.org/10.1016/B978-0-12-823137-1.00002-6.
5. Mahmoud Abd El Aleem Ali El-Remaily*, Ahmed M. Abu-Dief and Rafat M. El-Khatib, A robust synthesis and characterization of superparamagnetic CoFe2O4 nanoparticles as an efficient and reusable catalyst for green synthesis of some heterocyclic rings, DOI 10.1002/aoc.3536.
6. P. AjiUdhaya, M.Meena, Albumen Assisted Green Synthesis of NiFe2O4 Nanoparticles and Their Physico-Chemical Properties. ScienceDirect,Materials Today: Proceedings 9 (2019) 528–534.
7. Tahir Rasheed, Faran Nabeel, Muhammad Bilal, Hafiz M.N. Iqbal , Biogenic synthesis and characterization of cobalt oxide nanoparticles for catalytic reduction of direct yellow-142 and methyl orange dyes, 2019, Biocatalysis and Agricultural BiotechnologyVolume 19, May 2019, 101154, https://doi.org/10.1016/j.bcab.2019.101154.
8. KezhenQi, XiaohanXing, AmirZada, MengyuLi, QingWang, Shu-yuanLiu, HuaxiangLin, GuangzhaoWang, Transition metal doped ZnO nanoparticles with enhanced photocatalytic and antibacterial performances: Experimental and DFT studies, https://doi.org/10.1016/j.ceramint.2019.09.116.
9. Faniband, S. M., Vidyasagar, C., Jimenez, V., &Shridhar, A. (2022). Mechanistic insight into the photocatalytic degradation of organic pollutant and electrochemical behavior of modified MWCNTs/Cu-Co3O4 nanocomposite. ReactChemEng 01-26. https://doi 10.1039/d2re00117a.
10. Z Sheikhi Mehrabadi1, A Ahmadpour, NShahtahmasebiand M MBagheriMohagheghi, Synthesis and characterization of Cudoped cobalt oxide glucose detection. Sensing and Bio-Sensing Research https://doi.org/10.1016/j.sbsr.2019.100262nanocrystals as methane gas sensors, Article *in* PhysicaScripta · July 2011, https://doi:10.1088/0031-8949/84/01/015801.
11. MuslimaZahan, JibanPodder, Synthesis and Characterizations of Cu Doped Co3O4 Nanostructured Thin Films Using Spray Pyrolysis for Glucose Sensor Applications Volume 12, Issue 5, 2022, 6321 - 6335 https://doi.org/10.33263/BRIAC125.63216335
12. Selvanayaki R, Rameshbabu M, Muthupandi S, Razia M, SasiFlorence S, Ravichandran K, Prab ha K, Structural, optical and electrical conductivity studies of pure and Fe doped ZincOxide (ZnO) nanoparticlesVolume 49, Part 7, 2022, Pages 2628-2631, Materialstoday proceedings, https://doi.org/10.1016/j.matpr.2021.08.045.
13. I.S. Okeke , K.K. Agwu , A.A. Ubachukwu a , I.G. Madibad,e , M. Maazad,e , G.M. Whyte f , F. I. Ezema Impact of particle size and surface defects on antibacterial and photocatalytic activities of undoped and Mg-doped ZnO nanoparticles, biosynthesized using one-step simple process, (2021) https://doi.org/10.1016/j.vacuum.2021.110110.

14. ArshadMahmood, R.Rashid,U.Aziz, A.Shahn, ZahidAli, QaiserRaza, TanveerAshraf, Structural and opticalproperties of Zn1_xNixTe thin films prepared by electron beam evaporation technique, Progress in Natural Science: Materials International 25 (2015) 22–28.
15. Bansal V, Poddar P, Ahmad A, Sastry M (2006) Room-temperature biosynthesis of ferroelectric barium titanate nanoparticles. J Am ChemSoc 128:11958–11963. https ://doi.org/10.1021/ ja063 011m.
16. P. AjiUdhayaa, M.Meena, Albumen Assisted Green Synthesis of NiFe2O4 Nanoparticles and Their Physico-Chemical Properties, (2019), Materials Today: Proceedings 9 (2019) 528–534,
17. N. Pereira, S. Gonçalves, J.C. Barbosa, R. Gonçalves, C.R. Tubio , J. L. Vilas-
Vilela , C.M. Costa , S. Lanceros-Mendez, High dielectric constant poly(vinylidene fluoride trifluoroethylene-chlorofluoroethylene) for capacitive pressure and bending sensors. PolymerVolume 214, 1 February 2021, 123349, https://doi.org/10.1016/j.polymer.2020.123349**.**
18. **.** Z.-M. Dang, J.-K. Yuan, J.-W. Zha, T. Zhou, S.-T. Li, G.-H. Hu, Fundamentals, processes and applications of high-permittivity polymer–matrix composites, Prog. Mater. Sci. 57 (4) (2012) 660–723.
19. M. Meena et al Int. Journal of Engineering Research and Applications www.ijera.comISSN : 2248-9622, Vol. 4, Issue 5(Version 5), May 2014, pp.01-07.
20. Anantha, P &Hariharan, K 2012, 'Ac Conductivity analysis and dielectric relaxation behaviour of NaNO3-Al2O3 composites', Mater. Sci. Eng. B, vol. 121, pp. 12-19.
21. Sadaf Bashir Khan, Syed Irfan&Shern-Long Lee 2019, 'Influence of Zn+2 Doping on Ni-Based Nanoferrites; (Ni1−x ZnxFe2O4)', nanomaterials, 9, 1024.
22. NusratJahan, MdNazrul I. Khan &Jahirul I. Khandaker 2021, 'Exploration through Structural, Electrical, and Magnetic Properties of Al3+ Doped Ni−Zn−Co Nanospinel Ferrites', ACS Omega https://doi.org/10.1021/acsomega.1c04832.
23. K.M. Batoo, E.H. Raslan, S.F. Adil, I. Sharma, G. Kumar,Investigation of electrical, magnetic, and optical properties ofsilver substituted magnesium-manganese ferrite nanoparticles.
24. Gouda, GM &Nagendra, C 'Structural and electrical properties of mixed oxides of manganese and vanadium: a new semiconductor oxide thermistor material', Sens. Actuators, A vol. 155, pp. 263-271.
25. Chun Yan, L et al., 2011, 'Effect of sintering temperature on the microstructure and dielectric properties of SrTiO3', World Appl. Sci. J., vol. 14, pp. 1091-1094.
26. M.A. Dar, K.M. Batoo, V. Verma, W.A. Siddiqui, R.K. Kotnala, Synthesis and characterization of nano-sized pure and Al-doped lithium ferrite having high value of dielectric constant. J. Alloys Compds. 493, 553–560 (2010).
27. M. M. El-Desoky, M. A. Ali, G. Afifi, H. Imam, M. S. Al-Assiri, (2016), Effects of Annealing Temperatures on the Structural and Dielectric Properties of ZnO Nanoparticles. Silicon, DOI 10.1007/s12633-016-9445-5
28. H. Chouaibi Dr , K. KhirouniPr , E. DhahriPr, (2021), Enhanced dielectric performance of Dy - substituted YMn2O5 for high-frequency applications, Progress in Natural Science: Materials International, https://doi.org/10.1016/j.pnsc.2021.07.007
29. R. SakthiSudarSaravanan, M. Meena, D. Pukazhselvan, C. K. Mahadevan, Structural,optical and electrical characterization of Mn2+ and Cd2+ doped/co-doped PbSnanocrystals, *Journal of Alloys and Compounds* (2014), doi: http://dx.doi.org/10.1016/j.jallcom.2014.12.008.
30. T. Dippong, I.G. Deac, O. Cadar, E.A. Levei, L. Diamandescu, G. Borodi, Effect of Zn content on structural, morphological and magnetic behavior of ZnxCo1-xFe2O4/ SiO2nanocomposites. J. Alloys Compds. 792, 432–443 (2019).